13th World Conference on Earthquake Engineering
Vancouver, B.C., Canada
August 1-6, 2004
Paper No. 1761

SHEAR FORCE AND CAPACITY IN REINFORCED CONCRETE BEAM-COLUMN JOINTS WITH GOOD BOND ALONG BEAM AND COLUMN BARS

Shinji MORITA[1], Kazuhiro KITAYAMA[2], Shinji KISHIDA[3] and Takao NISHIKAWA[4]

SUMMARY

The effect of good bond along beam and column bars within a joint on shear strength in reinforced concrete interior beam-column joints was investigated. Five interior beam-column joint specimens with one-half scale were tested. The bond along beam and column bars within a joint and loading history were chosen as the test parameters. All specimens eventually failed in joint shear. To study on horizontal and vertical shear forces input to joint panel, concrete compressive stress distributions acting on beam and column critical sections were researched through measuring concrete normal strains by gauges stuck on beam and column surfaces. The depth of the concrete compressive zone at beam and column critical sections exceeded a half of the beam and column depth respectively. This means that all concrete compressive force at critical section is not necessarily introduced to joint panel as a shear force. The decrease in either horizontal or vertical joint shear force, which was computed using measured tensile forces of steel bars and accounting for non-contribution of the concrete compressive force to joint shear, resulted in the degradation of story shear force.

INTRODUCTION

At the Great Earthquake in Hanshin Awaji areas in 1995, a lot of severe damages were observed in reinforced concrete beam-column joints. Although provision to seismic design of beam-column joints was added after the great earthquake in AIJ Standard for Structural Calculation of Reinforced Concrete Structures [1], it is not based on the failure mechanism of beam-column joints.

Shear resistant mechanism of beam-column joints is currently studied focusing on the modeling for joint failure caused by deterioration of flexural resistant mechanism [2], [3], [4] and the stress transmission mechanism in a joint using finite element analysis [5], [6], [7]. These studies were not enough to explain the correlation of joint shear force with joint failure. The flexural resistant model by Shiohara [2] can explicate well the mechanism of joint failure without decrease in joint shear force. There is, however, different failure type of a joint panel from Shiohara model, which can be defined as shear failure caused

[1] Graduate Student, Tokyo Metropolitan University, Tokyo, Japan. Email:morita@ecomp.metro-u.ac.jp
[2] Associate Professor, Tokyo Metropolitan University, Tokyo, Japan. Email:kitak@ecomp.metro-u.ac.jp
[3] Research Associate, Tokyo Metropolitan University, Tokyo, Japan. Email:skishida@ecomp.metro-u.ac.jp
[4] Professor, Tokyo Metropolitan University, Tokyo, Japan. Email:tanishi@arch.metro-u.ac.jp

by the degradation of joint input shear force. It is necessary to grasp the influential parameters on the joint shear behavior.

In this paper, the concrete strains at the beam and column critical sections were measured in detail. Joint shear force was calculated considering the shape of concrete compressive stress block at the critical sections. Then five interior beam-column joint specimens without transverse beams nor slabs were tested to investigate the correlation of the bond along beam and column bars with the joint shear strength.

OUTLINE OF TEST

Specimens

Properties of specimens are listed in Table 1. Section dimensions and reinforcement details are shown in Figures 1 and 2. The five interior beam-column joint specimens with one-half scale were tested. Section dimensions and the specified concrete strength (18 N/mm^2) were common for all specimens. The beam width was equal to the column width for all specimens. The bond along beam and column bars within a joint and the loading history were chosen as the test parameters. Specimen M1 was control specimen. The bond along beam bars within a joint for Specimens M2, M3 and M4, and along column bars for Specimen M6 was improved by the increase in the surface area of the beam or column bar within a joint by welding the same diameter bars. The reinforcement details were identical for Specimens M2 and M3. The reversed cyclic load was applied at the top of the column for Specimens M1, M2, M4 and M6, whereas the monotonic load for Specimen M3. Hoops composed of four sets of 4-D13 were provided as joint lateral reinforcement for Specimen M4. Properties of the steel and the concrete are shown in Tables 2 and 3.

Table 1: Properties of specimens

Specimens	M1	M2	M3	M4	M6
Column axial load	none				
Column bar	Total bar : 16-D22, Hoops : 4-D10@60				
Beam bar	Top and bottom bar : 4-D25, Stirrups : 4-D10@60				
Joint Hoops	2-D6@80 2sets p_{wj}=0.16%			4-D13@40 4sets p_{wj}=2.51%	2-D6@80 2sets p_{wj}=0.16%
welded bar in a joint	none	beam bar			column bar
Loading path	reversed cyclic		monotonic	reversed cyclic	

p_{wj}:lateral reinforcement ratio in a joint

Table 2:Properties of steel bar

diameter	Yield stress $\sigma y(N/mm^2)$	Tensile strength $\sigma t(N/mm^2)$	Elongation ε_u (%)	Young's Modulus $Es(kN/mm^2)$
D6	344	485	27.3	186
D10	424	569	13.6	166
D13	429	593	13.7	184
D22	520	683	21.6	193
D25	520	674	14.2	192

E_s:Young's modulus was obtained by tensile test of steel bar

Table 3:Properties of concrete

specimens	Compressive strength $\sigma_B(N/mm^2)$	Tensile strength $\sigma t(N/mm^2)$	Young's modulus $Ec(kN/mm^2)$
M1	17.1	1.60	22.3
M2	18.2	1.76	23.6
M3	18.8	1.88	20.6
M4	20.6	1.55	22.3
M5	19.7	1.97	23.0
M6	19.4	1.93	23.5

Ec:Secant modulus at $1/4\sigma_B$

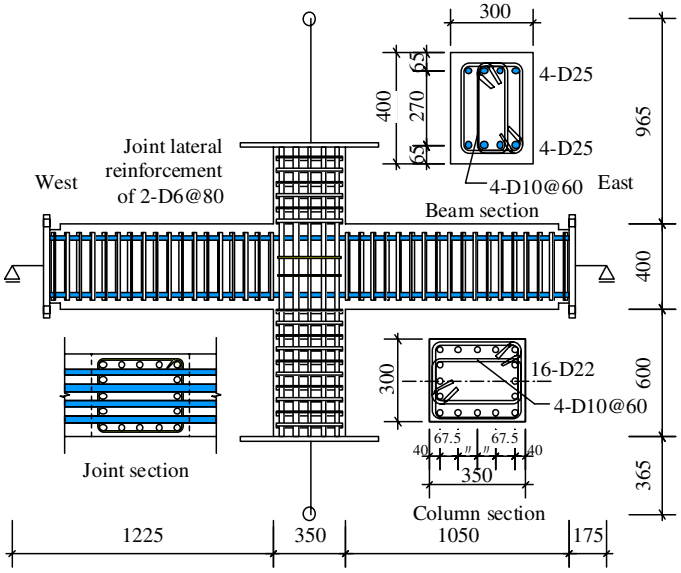

Figure 1: Section dimensions and reinforcement details

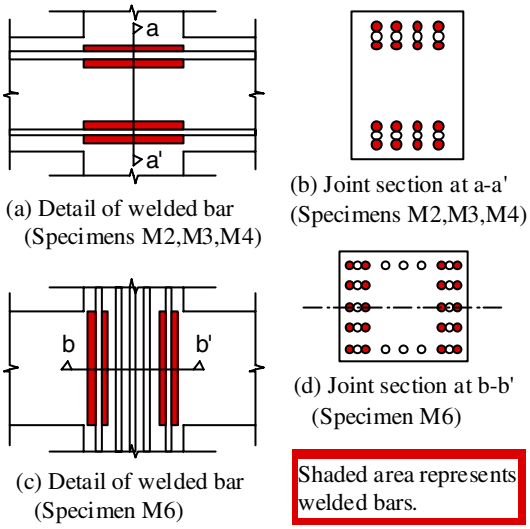

Figure 2: Details of welded bar in a joint

Loading Method

The beam ends were supported by horizontal rollers, while the bottom of the column was supported by mechanical hinge. The horizontal load was applied at the top of the column. The column axial load was not applied for the simplicity of the stress transmission in a joint panel. The lateral force was controlled by the story drift angle θ for 1 cycle of 1/400 radian, 2 cycles of 1/200, 1/100 and 1/50 radian, 1 cycle of 1/33 radian and to the end after 2 cycles of 1/25 radian.

TEST RESULTS

General Observations

The crack patterns after the story drift angle of 1/25 radian are shown in Figure 3. The diagonal shear cracks occurred in the joint panel for all specimens. The concrete compressive failure was observed in center of the joint panel for Specimen M1. However, the concrete compressive failure was observed in wide area of the joint panel for Specimen M2 with welded bars along beam bars in a joint. The diagonal cracks expanded to the beam and column hinge regions for Specimen M3 subjected to the monotonic horizontal load. Specimen M4 failed such as a direct shear along horizontal plane in the center of joint panel. The diagonal cracks expanded to the column hinge region for Specimen M6 with welded bars along column bars in a joint. Column bars did not yield for all specimens. A few beam bars yielded at the story drift angle of 1/25 radian only for Specimen M3. Therefore it was judged that the beam and column did not yield. All specimens eventually failed in a joint shear regardless of the beam and column bar bond condition.

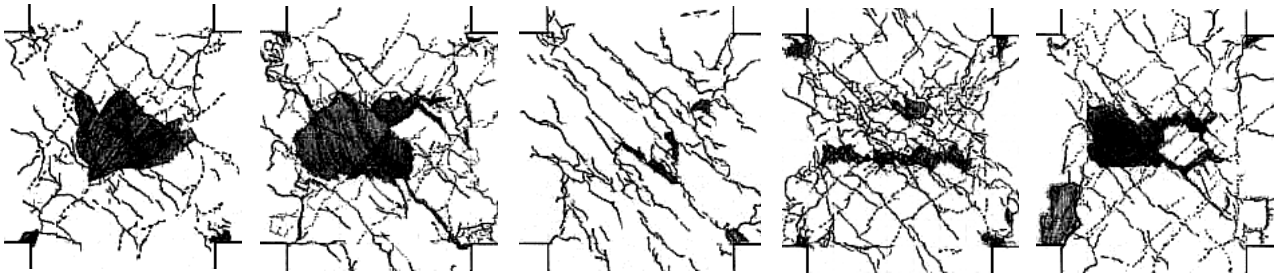

(a)Specimen M1 (b)Specimen M2 (c) Specimen M3 (d) Specimen M4 (e) Specimen M6

Figure 3: Crack patterns

Story Shear Force-Drift Relationships

The story shear force – drift relationships are shown in Figure 4. The maximum story shear force of Specimen M2 with welded bars along beam bars in a joint increased by 17%, and of Specimen M6 with welded bars along column bars in a joint increased by 14% comparing with that of Specimen M1. However, there was little influence of welded bars along column bars on maximum story shear force normalized by a concrete compressive strength σ_B for Specimens M1 and M6. The story drift angle at the maximum story shear force of Specimen M4 was larger than that of Specimen M2. However there was little difference among the maximum story shear forces. The maximum story shear force of Specimen M2 subjected to cyclic load was much the same as that of Specimen M3 subjected to monotonic load. The decline in the story shear force after the maximum story shear force of Specimen M3 was slight.

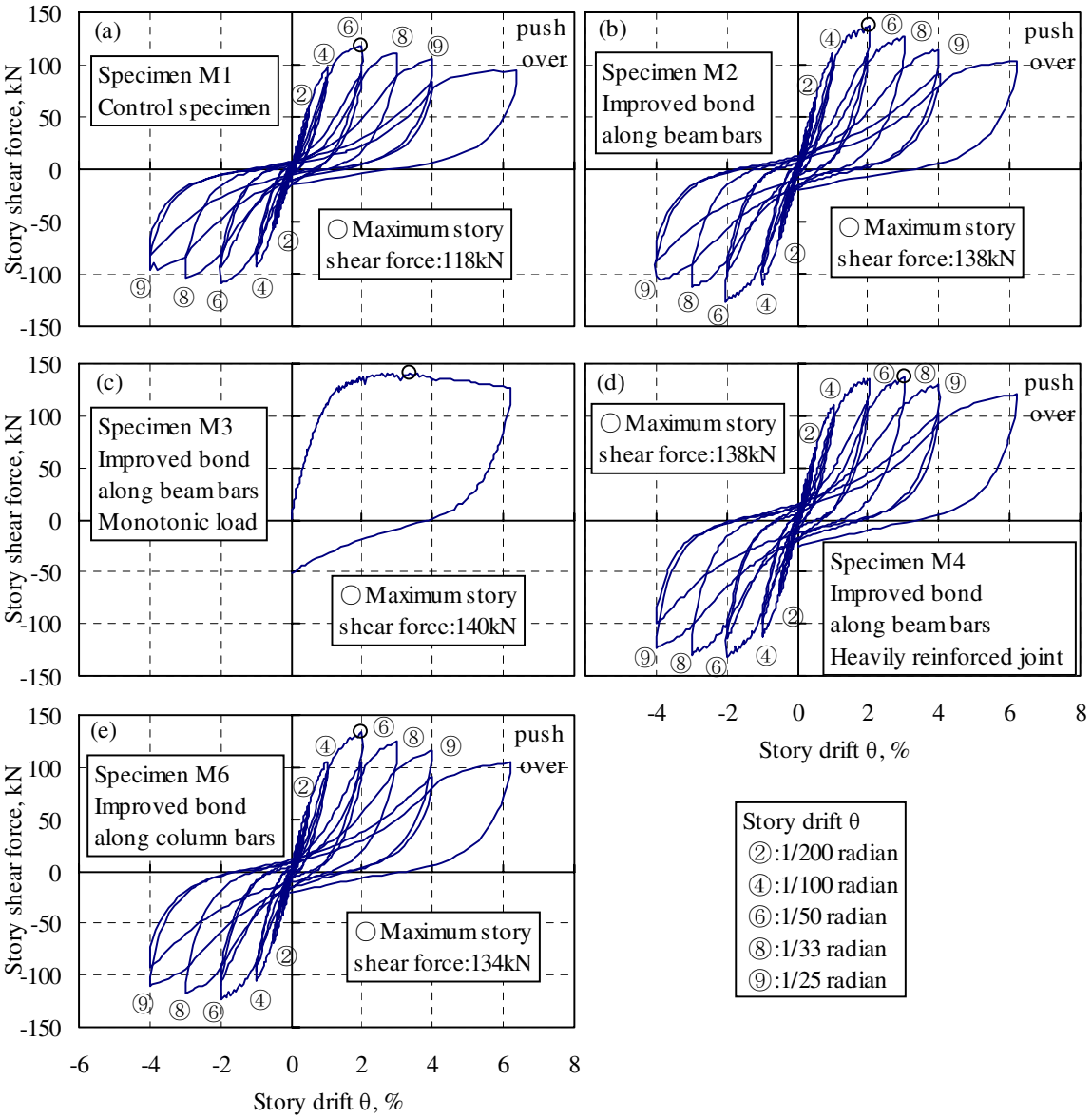

Figure 4: Story shear force – story drift relationships

DISCUSSION OF TEST RESULTS

Beam Bar Bond

The bond forces along a beam bar within a joint for all specimens are shown in Figure 5. The bond force was computed by the difference of the beam bar forces at opposite column faces. The bond forces along a beam bar decreased at the story drift angle of 1/50 radian for Specimen M1, and of 1/100 radian for Specimen M6. On the contrary, the bond forces of Specimens M2, M3 and M4 with welded bars along the beam bars increased successively. Then, it was judged that welded bars along beam bars improved the beam bar bond condition. The influence of the increase in lateral joint reinforcement on the beam bar bond was not observed. Since the bond forces of the specimens with welded bars along beam bars did not decrease even after the peak of the story shear force, the decrease in the story shear force is not attributed to the beam bar bond.

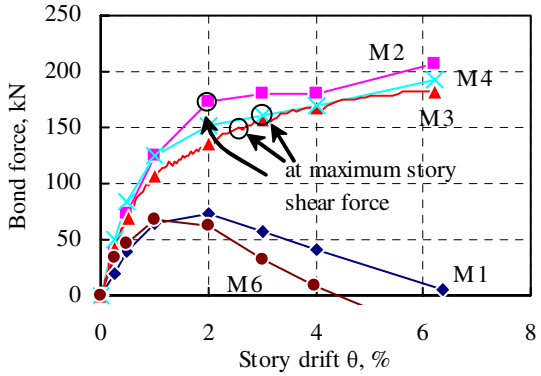

Figure 5: Bond force along beam bar

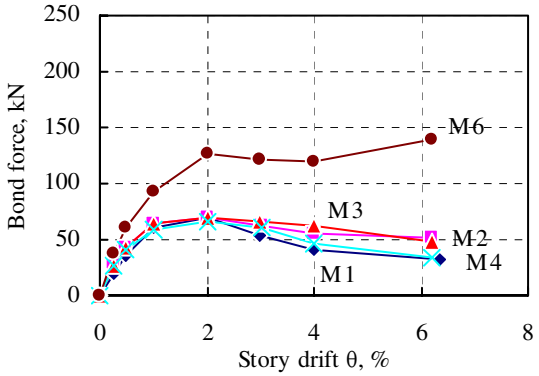

Figure 6: Bond force along column bar

Column Bar Bond

The bond forces along a column bar within a joint for all specimens are shown in Figure 6. The bond force was computed by the difference of the column bar forces at opposite beam faces. The bond forces along a column bar decreased at the story drift angle of 1/50 radian for Specimens M1, M2, M3 and M4. The bond forces along a column bar within a joint of Specimen M6 increased by 60% comparing with those of other specimens. Then, it was judged that welded bars along column bars improved the column bar bond condition. The decrease in the bond force along column bars caused the decay of the story shear force for Specimens M2, M3 and M4. Concrete at the beam critical section failed in compression by flexural moment after the peak of the story shear force for Specimen M6. Therefore the decrease in the bond force along beam bars caused the decay of the story shear force for Specimen M6.

Concrete Strains at Beam and Column Critical Section

The concrete normal strains at beam and column critical sections were measured by strain gauges for all specimens. The distributions of the concrete strain at the beam critical section for Specimens M1, M3 and M6 are shown in Figure 7. The concrete strain ε_c at the compressive strength obtained by cylinder tests was drawn by a dashed line in Figure 7. The depth of the concrete compressive region at beam critical section was approximately equal to beam full depth. The large compressive strain occurred at the top fiber in tension because of residual accumulation of compressive strain due to cyclic load reversals. The distribution of the concrete strain formed a triangle for Specimen M3 subjected to monotonic load. If residual accumulation of compressive strain could be taken away, the distributions of the concrete compressive strain would also form a triangle for the specimens subjected to the reversed cyclic load. The compressive strain at the bottom fiber exceeded the strain of ε_c at the story drift angle of 1/50 radian.

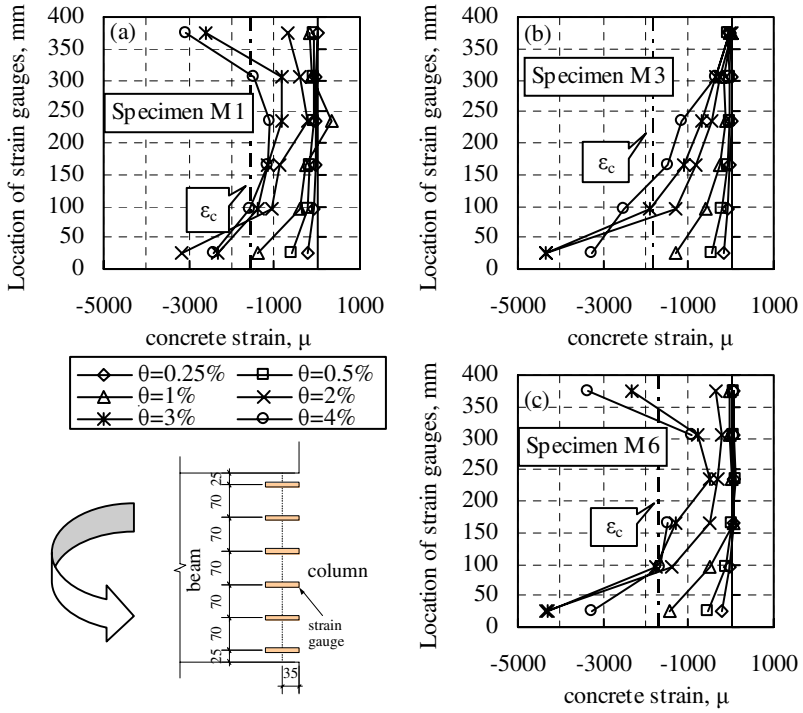

Figure 7: Strain distributions of concrete at beam critical section

Forces on both beam critical sections induced by the beam moment M_b is shown in Figure 8(a), and the distribution of confining force to the horizontal expansion in joint panel is shown in Figure 8(b). Flexural cracks occurred in critical sections at the story drift angle of 1/400 radian. Since shear force acts simultaneously on the beam critical section in addition to flexural moment, the confining force can be carried across the flexural crack by aggregate interlocking. Then the confining force decreases gradually toward the top (or bottom) fiber in tension because of wide crack opening as shown in Figure 8(c). Therefore, the distribution of the concrete compressive stress at beam critical section would result in a triangle by the superposition of both concrete stress conditions shown in Figures 8(a) and 8(c).

The distributions of the concrete strain at the column critical section for Specimens M1, M3 and M6 are shown in Figure 9. The depth of the concrete compressive region was approximately equal to column full depth. The distribution of the compressive stress at column critical section would also form a triangle due to the same reason as the case of a beam.

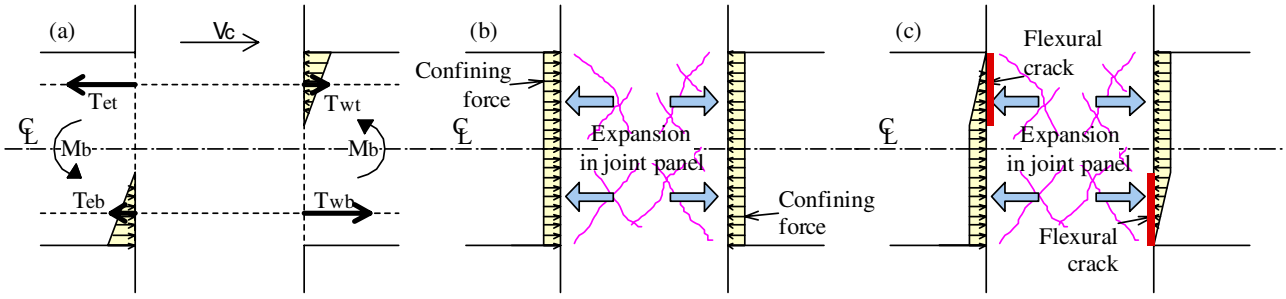

Figure 8: Distribution of concrete compressive stress

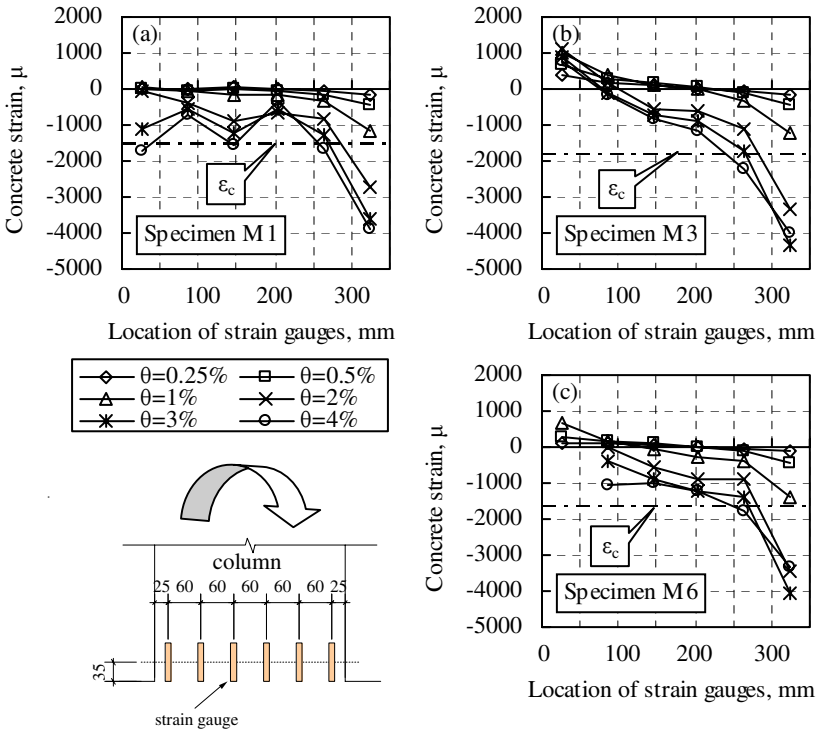

Figure 9: Strain distributions of concrete at column critical section

Joint Shear Force

Calculation of Horizontal Joint Shear Force

The stresses acting on the beam critical section are assumed as shown in Figure 10, where the distributions of the concrete compressive stress at both beam critical sections are congruent. The distribution of the concrete compressive stress was assumed to form a trapezoid by taking account of crushed concrete zone. The maximum concrete compressive stress was taken equal to 0.85 σ_B according to the provisions by ACI Committee 318 [8], where σ_B is concrete compressive strength by cylinder tests. Notation *x* is the depth of crushed compression zone. Notations T_{et} and T_{eb} are beam bar force at east top and bottom respectively, notations T_{wt} and T_{wb} are beam bar force at west top and bottom respectively, notations C_{ce} and C_{cw} are resultant concrete force at east and west beam section respectively, notation D_b is beam depth and notation V_c is story shear force. Maximum horizontal joint shear force develops mathematically on the horizontal center section in a joint panel. The horizontal joint shear force is obtained by following equation.

$$V_{jh} = T_{et} + \alpha_b \cdot C_{cw} - \beta_b \cdot C_{ce} - T_{wt} - V_c \tag{1}$$

where coefficient α_b is the ratio of concrete compressive force acting above center axis to resultant force C_{cw} on west beam critical section, and coefficient β_b is the ratio of concrete compressive force acting above center axis to resultant force C_{ce} on east beam critical section. The sum of coefficients α_b and β_b becomes unity due to symmetrical stress distribution of concrete on both beam critical sections. The following equations can be obtained from the equilibrium of forces at beam critical sections.

$$C_{cw} = T_{wt} + T_{wb} \tag{2}$$

$$C_{ce} = T_{et} + T_{eb} \tag{3}$$

The following equation is obtained by substituting Eqs.(2) and (3) into Eq.(1).

$$
\begin{aligned}
V_{jh} &= T_{et} + \alpha_b (T_{wt} + T_{wb}) - \beta_b (T_{et} + T_{eb}) - T_{wt} - V_c \\
&= T_{et} + (1 - \beta_b) \cdot (T_{wt} + T_{wb}) - \beta_b (T_{et} + T_{eb}) - T_{wt} - V_c \\
&= T_{et} + T_{wb} - V_c - \beta_b (T_{wt} + T_{wb} + T_{et} + T_{eb})
\end{aligned} \tag{4}
$$

The coefficient β_b is obtained by following equations.

$$
\beta_b = \begin{cases} \dfrac{D_b^{\,2}}{4(D_b^{\,2} - x^2)} & for\ 0 \le x < \dfrac{D_b}{2} \\ \dfrac{x}{x + D_b} & for\ \dfrac{D_b}{2} \le x < D_b \end{cases} \tag{5}
$$

The coefficient β_b – the depth of crushed compression zone x relationships are shown in Figure 11. The coefficient β_b of Specimen M1 was plotted in Figure 11. The horizontal joint shear stresses – joint shear distortion angle relationships are shown in Figure 12. The joint shear stresses were computed by dividing the joint shear force by the effective sectional area of the joint panel defined as the product of the beam width (equal to the column width) and the column depth. The depth of crushed compression zone x was decided as the point where the line of strain distribution crosses vertical line of ε_c in Figure 7. Beam bar force was computed from the measured strains at the critical section through Ramberg-Osgood Model. Average joint shear strength computed according to the provisions by Architectural Institute of Japan [9] are drawn by dashed line in Figure 12. The horizontal joint shear stresses obtained by Eq.(4) for Specimens M1 and M6 with deteriorating beam bar bond were by 21 to 28% smaller than the average joint shear strength obtained by the provisions by Architectural Institute of Japan [9]. The maximum joint shear force obtained by Eq.(4) for Specimens M1 and M6 were approximately equal to the lower limit of the joint shear strength computed by multiplying the average joint shear strength by 0.85. On the contrary, the joint shear stresses obtained by Eq.(4) for Specimens M2, M3 and M4 with improved beam bar bond increased to the end of the test. Therefore, the behavior of beam bar bond provided great influence on the horizontal joint shear force.

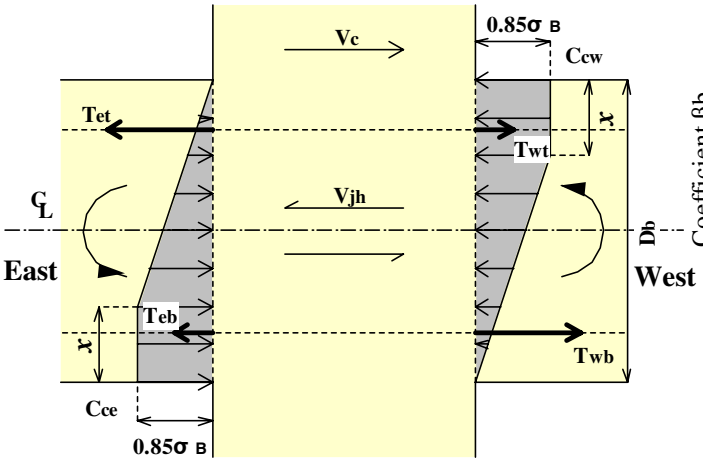

Figure 10: Stress condition at beam critical section

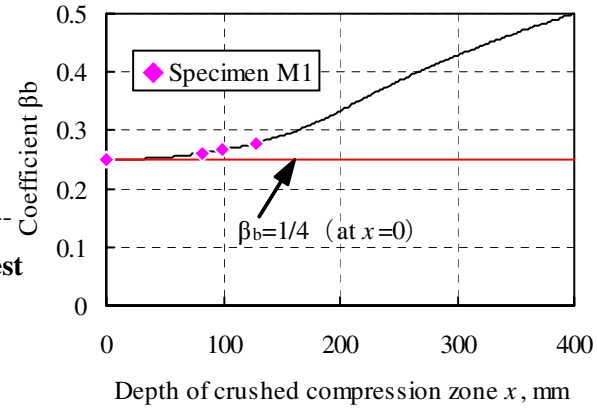

Figure 11: Coefficient β_b – depth of crushed compression zone x relationships

Calculation of Vertical Joint Shear Force

The stresses acting on the column critical section are shown in Figure 13, which were assumed in the same manner as beam section. Notations T_{te1}, T_{te2}, T_{tm}, T_{tw2} and T_{tw1} are column bar forces at top critical section, notations T_{be1}, T_{be2}, T_{bm}, T_{bw2} and T_{bw1} are column bar forces at bottom critical section, notation C_{ct} and C_{cb} are resultant force at top and bottom column section respectively, notation D_c is column depth and notations V_{be} and V_{bw} are east and west beam shear force respectively. Maximum vertical joint shear

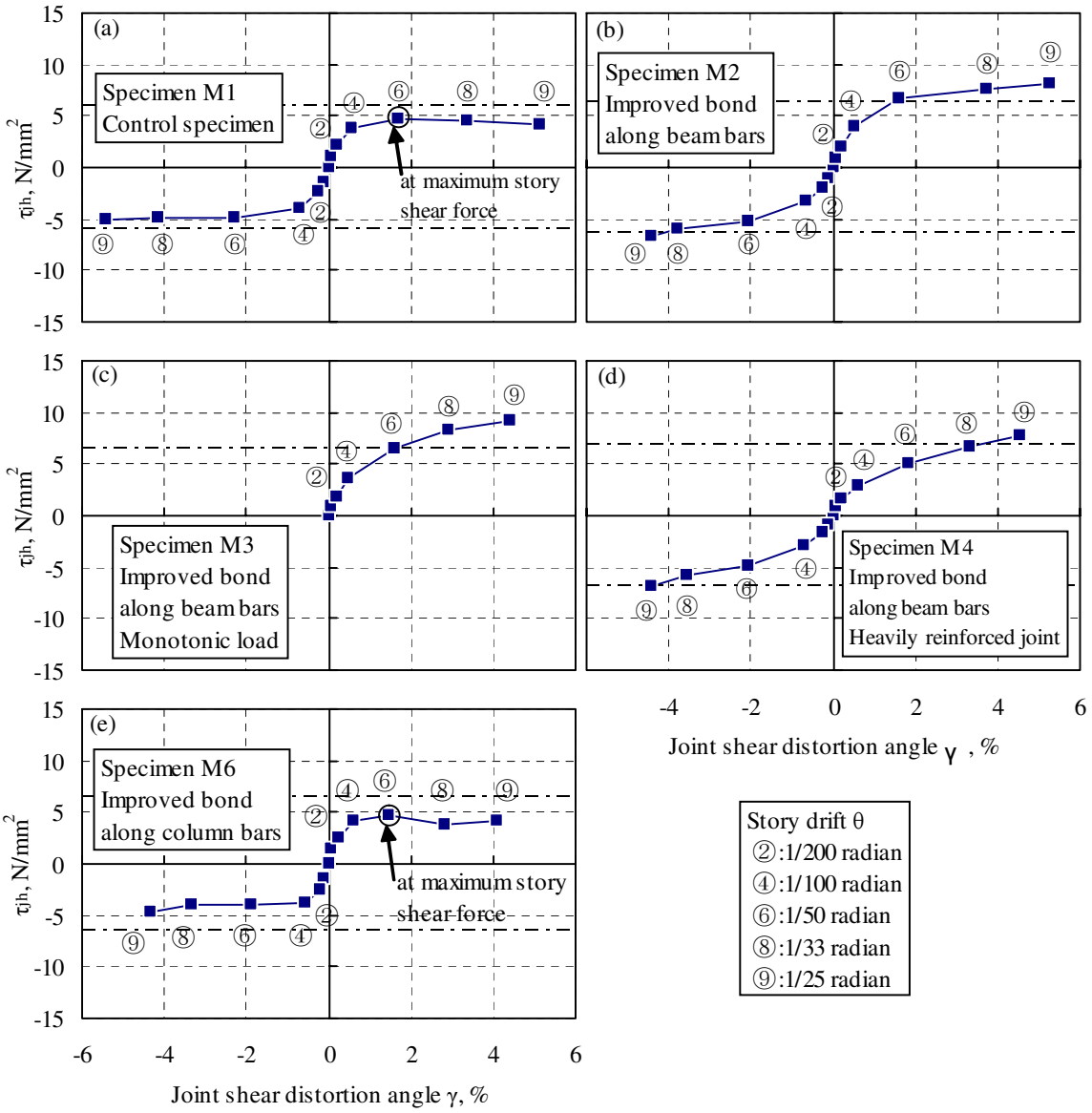

Figure 12: Horizontal joint shear stress – joint shear distortion relationships

force develops mathematically on the vertical center section in a joint panel. The vertical joint shear force is obtained by following equation.

$$V_{jv} = T_{et1} + T_{te2} + \alpha_c \cdot C_{cb} - T_{be1} - T_{be2} - \beta_c \cdot C_{ct} - V_{be} \tag{6}$$

where coefficient α_c is the ratio of concrete compressive force acting on the east side of center axis to resultant force C_{cb} on bottom column critical section, and coefficient β_c is the ratio of concrete compressive force acting on the east side of center axis to resultant force C_{ct} on top column critical section. The sum of coefficients α_c and β_c becomes unity. The following equations can be obtained from the equilibrium of forces at column critical section.

$$C_{ct} = T_{te1} + T_{te2} + T_{tm} + T_{tw2} + T_{tw1} \tag{7}$$

$$C_{cb} = T_{be1} + T_{be2} + T_{bm} + T_{bw2} + T_{bw1} \tag{8}$$

The following equation is obtained by substituting Eqs.(7) and (8) into Eq.(6).

$$
\begin{aligned}
V_{jv} &= T_{te1} + T_{te2} + \alpha_c (T_{be1} + T_{be2} + T_{bm} + T_{bw2} + T_{bw1}) - \beta_c (T_{te1} + T_{te2} + T_{tm} + T_{tw2} + T_{tw1}) - V_{be} \\
&= T_{te1} + T_{te2} + (1 - \beta_c) \cdot (T_{be1} + T_{be2} + T_{bm} + T_{bw2} + T_{bw1}) - \beta_c (T_{te1} + T_{te2} + T_{tm} + T_{tw2} + T_{tw1}) - V_{be} \\
&= T_{te1} + T_{te2} + T_{bm} + T_{bw2} + T_{bw1} - V_{be} - \beta_c (T_{be1} + T_{be2} + T_{bm} + T_{bw2} + T_{bw1} + T_{te1} + T_{te2} + T_{tm} + T_{tw2} + T_{tw1})
\end{aligned} \tag{9}
$$

The coefficient β_c is obtained by following equations.

$$
\beta_c = \begin{cases} \dfrac{D_c^{\,2}}{4(D_c^{\,2} - x^2)} & for\ 0 \le x < \dfrac{D_c}{2} \\ \dfrac{x}{x + D_c} & for\ \dfrac{D_c}{2} \le x < D_c \end{cases} \tag{10}
$$

The coefficient β_c – the depth of crushed compression zone x relationships are shown in Figure 14. The coefficient β_c for Specimen M1 was plotted in Figure 14. The vertical joint shear stresses – joint shear distortion angle relationships are shown in Figure 15. The joint shear stresses were computed by dividing the joint shear force by the effective sectional area of the joint panel defined as the product of the column width and the beam depth. The depth of crushed compression zone x and column bar force were decided by the same manner as beam section. Average joint shear strength computed according to the provisions by Architectural Institute of Japan [9] are drawn by dashed line in Figure 15. The vertical joint shear stresses obtained by Eq.(9) for Specimens M1, M2, M3 and M4 with deteriorating column bar bond were by 7.5 to 19% smaller than the average joint shear strength computed according to the provisions by Architectural Institute of Japan [9]. The joint shear strengths obtained by Eq.(9) for Specimens M1, M2, M3 and M4 were approximately equal to the lower limit of the joint shear strength computed by multiplying the average joint shear strength by 0.85. On the contrary, the joint shear stress obtained by Eq.(9) for Specimen M6 with improved column bar bond increased to the end of the test. Therefore, the behavior of column bar bond had great influence on the vertical joint shear force.

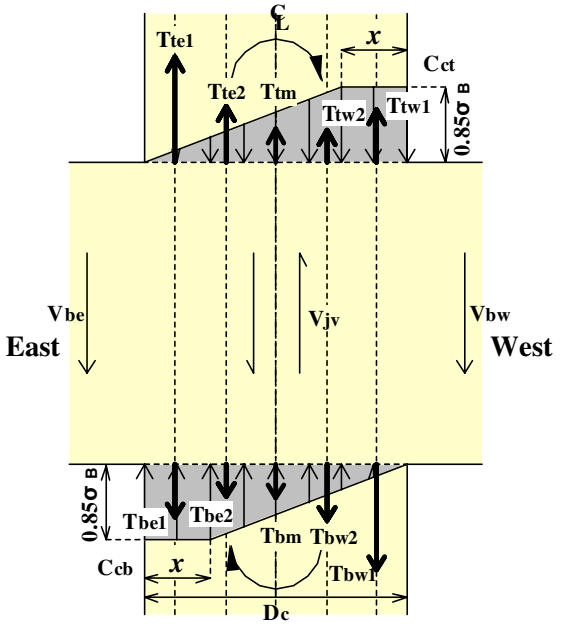

Figure 13: Stress condition at column critical section

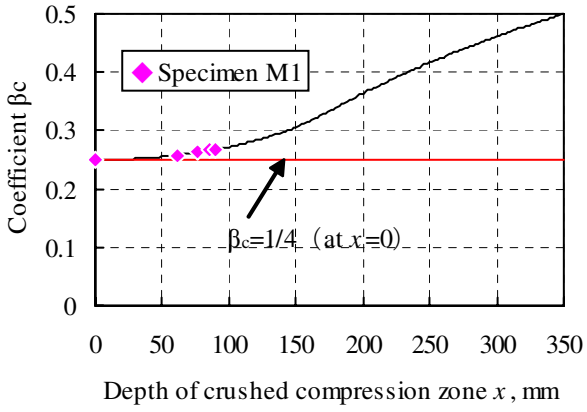

Figure 14: Coefficient β_c – depth of crushed compression zone x relationships

Evaluation of Joint Shear Capacity

The horizontal joint shear stresses of Specimens M1 and M6 with deteriorating beam bar bond decreased after the peak of story shear force. Similarly the vertical joint shear stresses of Specimens M1, M2, M3 and M4 with deteriorating column bar bond decreased after the peak of story shear force. Notice that the

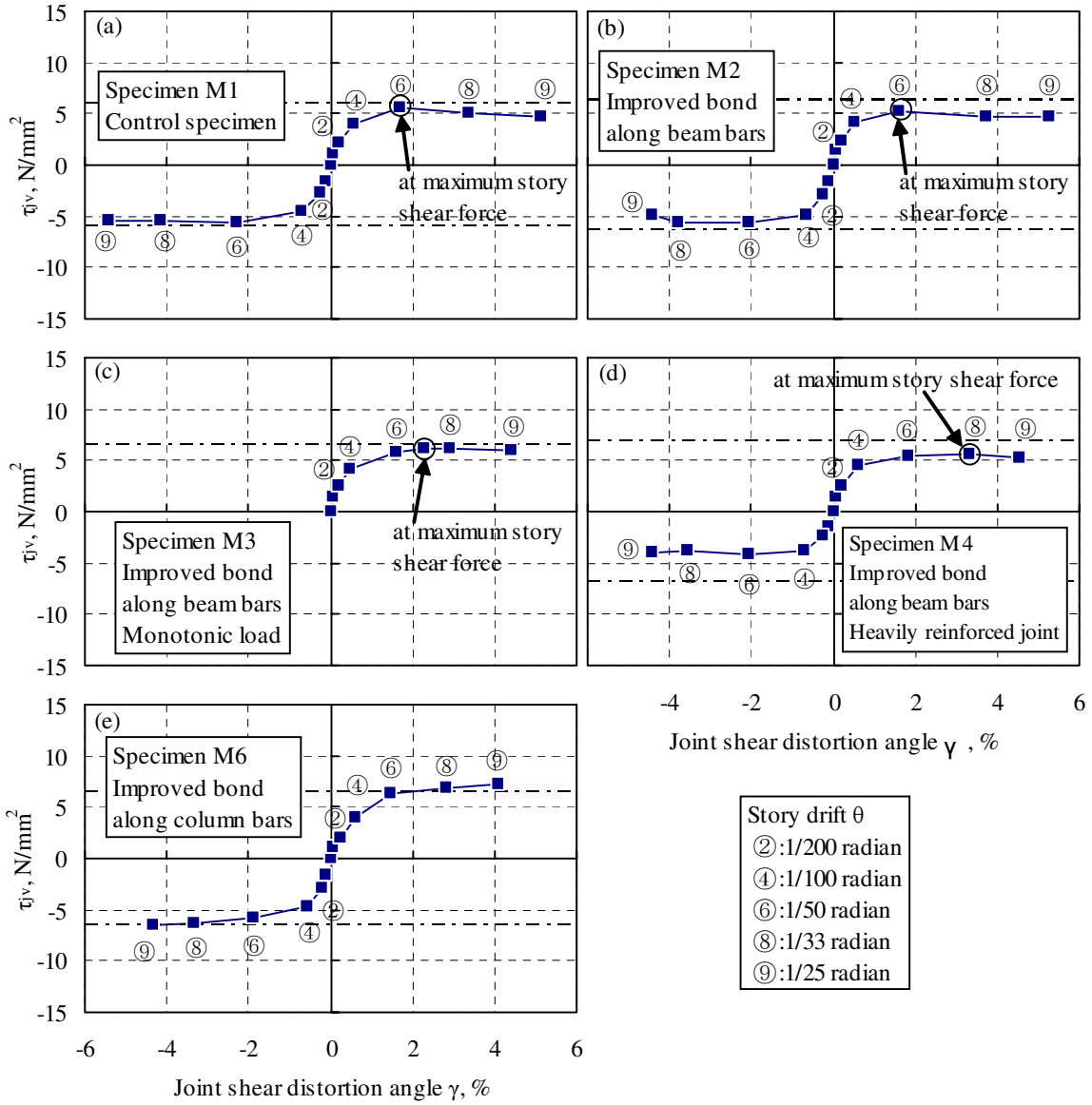

Figure 15: Vertical joint shear stress – joint shear distortion relationships

decrease in either horizontal or vertical joint shear force caused the degradation of story shear force as in the case of Specimen M6 or Specimens M2, M3 and M4.

The joint shear capacity was decided by accepting horizontal or vertical maximum joint shear forces whichever is smaller. The joint shear capacities and the lower limit of the joint shear strength computed

Table 4: Joint shear capacities

Specimen	τ_{jh}, N/mm^2	τ_{jv}, N/mm^2	Joint shear capacity τ_j, N/mm^2	Lower limit of joint shear strenth[9] τ_{ul}, N/mm^2	τ_j / τ_{ul}
M1	4.77	5.58	4.77	5.13	0.93
M2	–	5.66	5.66	5.36	1.06
M3	–	6.13	6.13	5.48	1.12
M4	–	5.59	5.59	5.86	0.95
M6	4.72	–	4.72	5.60	0.84

according to the provisions by Architectural Institute of Japan [9] for all specimens are listed in Table 4. If the skeleton curve of joint shear force did not have local maxima, notation '–' was described in Table 4. The joint shear capacity could be evaluated appropriately by using the lower limit of the joint shear strength for all specimens.

CONCLUSIONS

The conclusions obtained in this study can be summarized as follows.

(1) The maximum story shear force increased by 17% for the specimen with improved beam bar bond and 14% for the specimen with improved column bar bond.
(2) The distributions of the concrete compressive stress on beam and column critical sections resulted in a triangle due to flexural crack and shear force.
(3) The behavior of beam and column bar bond provided great influence on horizontal and vertical joint shear force respectively. The decrease in the horizontal and/or vertical joint shear caused the decay of the story shear force.
(4) The joint shear capacity was decided by accepting horizontal or vertical maximum joint shear forces whichever is smaller. The joint shear capacity could be evaluated appropriately by using lower limit of the joint shear strength computed according to the provisions by Architectural Institute of Japan [9].

REFERENCES

1. Architectural Institute of Japan, "AIJ Standard for Structural Calculation of Reinforced Concrete Structures –Based on Allowable Stress Concept–", 1999.
2. Kusuhara,F and H.Shiohara, "Re-evaluation of Joint Shear Tests of R/C Beam-Column Joints Failed in Shear," Proceedings of the Japan Concrete Institute, Vol.19, No.2, pp.1005-1010, 1997, (in Japanese).
3. Kishikawa,S and H.Shiohara, "Relation of Joint Shear and Joint Shear Failure in Reinforced Concrete Beam-Column Joint," Proceedings of the Japan Concrete Institute, Vol.20, No.3, pp.523-528, 1998, (in Japanese).
4. Shiohara,S, S.Zaid and S.Kotani, "Interaction of Joint Shear and Anchorage Force in Beam-Column Connections," Proceedings of the Japan Concrete Institute, Vol.23, No.3, pp.355-360, 2001, (in Japanese).
5. Sunai,T, Y.Goto and O.Joh, "3-Dimensional Finite Element Analysis on Seismic Behavior of RC Interior Beam-Column Joints," Proceedings of the Japan Concrete Institute, Vol.21, No.3, pp.643-648, 1999, (in Japanese).
6. Dachang,Z, H.Noguchi and T.Kashiwazaki, "The Analytic Study on a Joint Reinforcing Detail Improving Joint Capacity of R/C Interior Beam-Column Joint with Plane Finite Element Method," Proceedings of the Japan Concrete Institute, Vol.23, No.3, pp.403-408, 2001, (in Japanese).
7. Noguchi,H, D.Zhnang and T.Kashiwazaki, "Three-Dimensional Finite Element Analysis of RC Beam-Column Joints Reinforced by New Reinforcing Way," Proceedings of the Japan Concrete Institute, Vol.24, No.2, pp.397-402, 2002, (in Japanese).
8. ACI Committee 318, "Building Code Requirements for Structural Concrete and Commentary, ACI318-95", 1995.
9. Architectural Institute of Japan, "Design Guidelines for Earthquake Resistant Reinforced Concrete Buildings Based on Inelastic Displacement Concept," 1999.